⌘ *Author's Choice*

THE JOURNAL OF BIOLOGICAL CHEMISTRY VOL. 287, NO. 12, pp. 9633–9639, March 16, 2012


# Kinetic Equivalence of Transmembrane pH and Electrical Potential Differences in ATP Synthesis*[S]

Received for publication, December 23, 2011, and in revised form, January 12, 2012 Published, JBC Papers in Press, January 17, 2012, DOI 10.1074/jbc.M111.335356

**Naoki Soga[‡], Kazuhiko Kinosita, Jr.[‡1], Masasuke Yoshida[§¶], and Toshiharu Suzuki[§]**

*From the [‡]Department of Physics, Faculty of Science and Engineering, Waseda University, 3-4-1 Okubo, Shinjuku-ku, Tokyo 169-8555, Japan, the [§]International Cooperative Research Project (ICORP) ATP Synthesis Regulation Project, Japan Science and Technology Agency, 2-3-6 Aomi, Koto-ku, Tokyo 135-0064, Japan, and the [¶]Department of Molecular Bioscience, Kyoto Sangyo University, Kamigamo-Motoyama, Kyoto 603-8555, Japan*

**Background:** ATP synthesis is driven by the combination of transmembrane electrical potential and pH difference.
**Results:** Either electrical potential or pH difference can drive synthesis even when the other opposes.
**Conclusion:** The synthesis rate depends on the algebraic sum of the two, irrespective of the individual magnitudes and signs.
**Significance:** Comprehensive data sets directly attest to kinetic equivalence of the two.

**ATP synthase is the key player of Mitchell's chemiosmotic theory, converting the energy of transmembrane proton flow into the high energy bond between ADP and phosphate. The proton motive force that drives this reaction consists of two components, the pH difference (ΔpH) across the membrane and transmembrane electrical potential (Δψ). The two are considered thermodynamically equivalent, but kinetic equivalence in the actual ATP synthesis is not warranted, and previous experimental results vary. Here, we show that with the thermophilic *Bacillus* PS3 ATP synthase that lacks an inhibitory domain of the ϵ subunit, ΔpH imposed by acid-base transition and Δψ produced by valinomycin-mediated $K^+$ diffusion potential contribute equally to the rate of ATP synthesis within the experimental range examined (ΔpH −0.3 to 2.2, Δψ −30 to 140 mV, pH around the catalytic domain 8.0). Either ΔpH or Δψ alone can drive synthesis, even when the other slightly opposes. Δψ was estimated from the Nernst equation, which appeared valid down to 1 mM $K^+$ inside the proteoliposomes, due to careful removal of $K^+$ from the lipid.**

The $F_oF_1$-ATP synthase is a ubiquitous enzyme that synthesizes ATP from ADP and inorganic phosphate ($P_i$) using the electrochemical potential difference of protons (or $Na^+$ in some species) across a membrane, referred to as the proton motive force (pmf)[2] (1–5). The $F_o$ portion is embedded in a membrane, and its simplest subunit composition (in bacteria) is $ab_2c_{10-15}$ (6). The soluble $F_1$ portion with the minimal composition of $\alpha_3\beta_3\gamma\delta\epsilon$ contains three catalytic sites for ATP synthesis (or hydrolysis in the reverse reaction) at $\beta$-$\alpha$ interfaces (7). Rotational catalysis has been proposed (8, 9) and evidenced: in isolated $F_1$, ATP hydrolysis drives rotation of the central $\gamma$ subunit against the $\alpha_3\beta_3$ ring (10), and reverse rotation forced by an external force leads to ATP synthesis (11, 12). In the whole synthase, the reverse rotation for ATP synthesis is considered to be forced by the proton-powered $F_o$ motor, and proton-driven rotation of the ring of *c* subunits against the *a* subunit has indeed been demonstrated (13) in addition to the proton-driven rotation of $\gamma$ (14) and $\epsilon$ (15) in a membrane-reconstituted synthase. The current view is that the *c*-ring and the $\gamma\epsilon$ subunits constitute a common rotor that rotates against $ab_2\alpha_3\beta_3\delta$; in the tight coupling scenario, every proton that flows through the *a*-*c* interface in the direction of $F_o$ to $F_1$ rotates the *c*-ring by one *c* subunit in the synthesis direction, and each ATP hydrolyzed in $F_1$ drives opposite rotation by 120°, pumping protons backward. The actual direction of rotation depends on whether $F_o$ or $F_1$ wins, or on the balance between the two opposing forces produced by proton flow and ATP hydrolysis. Steigmiller *et al.* (16) have demonstrated experimentally that the two forces can precisely be balanced in ATP synthase.

The proton motive force that drives the synthesis of ATP consists of two components: $\text{pmf} = \Delta\psi + 2.30\,(k_BT/e)\,\Delta\text{pH}$, where $\Delta\psi$ is the transmembrane electrical potential, ΔpH is the pH difference across the membrane, $k_B$ is the Boltzmann constant, $T$ is the absolute temperature, and $e$ is the proton charge ($2.30k_BT/e$ ~60 mV at room temperature). The two terms are thermodynamically equivalent (17), but kinetic equivalence in an actual ATP synthase is not warranted. The two should in principle be equivalent in the core reaction, but pH and membrane potential could affect the enzyme in various ways. Kinetic equivalence of ΔpH and $\Delta\psi$ has been proposed for $F_oF_1$ from *Wolinella succinogenes*, *Rhodospirillum rubrum*, and spinach chloroplast (18–21) and for the $Na^+$-driven $F_oF_1$ of *Propionigenium modestum* (22). With *Rhodobacter capsulatus* (23) and particularly with *Escherichia coli* $F_oF_1$ (24, 25), in contrast, ΔpH and $\Delta\psi$ display different kinetics. The apparent non-equiva-

* This work was supported in part by grants-in-aid for Specially Promoted Research by the Japan Society for the Promotion of Science (to K. K.), in part by the ATP Synthesis Regulation Project by the Japan Science and Technology Agency (to M. Y.), and in part by a research fellowship from the Japan Society for the Promotion of Science (to N. S.).
⌘ *Author's Choice*—Final version full access.
[S] This article contains supplemental Figs. S1–S4 and an additional reference.
[1] To whom correspondence should be addressed: Dept. of Physics, Faculty of Science and Engineering, Waseda University, 3-4-1 Okubo, Shinjuku-ku, Tokyo 169-8555, Japan. Tel.: 81-3-5952-5871; E-mail: kazuhiko@waseda.jp.
[2] The abbreviations used are: pmf, proton motive force; ΔpH, pH difference across the membrane; $\Delta\psi$, transmembrane electrical potential; Tricine, *N*-[2-hydroxy-1,1-bis(hydroxymethyl)ethyl]glycine; $[K^+]_{in}$, potassium concentration inside liposomes; $[K^+]_{out}$, potassium concentration outside liposomes; $pH_{in}$, pH inside liposomes; $pH_{out}$, pH outside liposomes; $TF_oF_1$, $F_oF_1$-ATP synthase from thermophilic *Bacillus* PS3.

lence, however, could be ascribed to the activation of the enzyme where ΔpH and Δψ may exert different effects (23, 24). A systematic investigation is awaited for the $F_oF_1$ of thermophilic *Bacillus* PS3 ($TF_oF_1$), of which the $F_1$ part has contributed much to the understanding of the mechanism of coupling between rotation and hydrolysis/synthesis of ATP (4, 5, 26).

Recently, we have developed a proteoliposome system for $TF_oF_1$ that shows a reasonable rate of synthesis at room temperature with high reproducibility (27). To facilitate activation at least partially, we removed the inhibitory domain (27, 28) of the ε subunit. Using this system, we inquire here whether ΔpH and Δψ are kinetically equivalent in $TF_oF_1$ and, if so, over which ranges. We show that either ΔpH or Δψ alone suffices for ATP synthesis and that the two contribute equally to the rate of synthesis for any combination of ΔpH in the range of −0.3 to 2.2 and Δψ between −30 and 140 mV (pmf up to 250 mV).

## EXPERIMENTAL PROCEDURES

*Preparation of $TF_oF_1$*—The $TF_oF_1$ we used in this work was a mutant, termed $TF_oF_1^{\epsilon\Delta c}$ in previous studies (27, 28), that has a $His_{10}$ tag at the N terminus of each β subunit and that lacks the inhibitory C-terminal domain of the ε subunit. $TF_oF_1$ was expressed in an $F_oF_1$-deficient *E. coli* strain DK8 by an expression plasmid pTR19-ASDS-εΔc and purified as described (27, 29) with the following modifications. At the final stage, the elution from the ion-exchange column (ResourceQ, GE Healthcare) showed four closely located protein peaks, of which the first and third gave higher rate of ATP synthesis. We thus mixed the two fractions and replaced the medium with 20 mM HEPES, 0.2 mM EDTA, and 0.15% *n*-decyl-β-D-maltoside (Dojindo), pH adjusted with NaOH to 7.5, in a centrifugal concentrator with a cut-off molecular mass of 50 kDa (Amicon Ultra, Millipore). The purified $TF_oF_1$ at 30 μg/μl was aliquoted into 25 μl, frozen by liquid $N_2$, and stored at −80 °C until use. The molar concentration of $TF_oF_1$ was determined from absorbance with the molar extinction coefficient at 280 nm of 253,000 $M^{-1}$ $cm^{-1}$. Protein mass was calculated by taking the molecular mass of $TF_oF_1$ as 530 kDa.

*Removal of $K^+$ from Lipid*—The lipid for reconstitution was crude soybean L-α-phosphatidylcholine (P5638, Type II-S, Sigma), which contained a significant amount of $K^+$. First, we washed the lipid with acetone (30) and suspended it at 40 mg/ml in LW buffer (40 mM Tricine, 40 mM MES, 50 mM NaCl, 5 mM $MgCl_2$, and 1 mM DTT, pH adjusted with NaOH to 8.0). The suspension was incubated for 30 min with gentle stirring to allow the lipid to swell. We then sonicated the suspension with a tip-type sonicator (UR-20P, Tomy Seiko) for 30 s. After a 4-fold dilution with LW buffer, we centrifuged the lipid at 235,000 × *g* for 90 min at 4 °C and resuspended it at 10 mg/ml in LW buffer. The lipid suspension was frozen with liquid $N_2$ and thawed at 25 °C. The centrifugation, resuspension, and freezing/thawing were repeated three times. After fourth centrifugation, we suspended the lipid in R buffer (40 mM Tricine, 40 mM MES, and 5 mM $MgCl_2$, pH adjusted with NaOH to 8.0) at 10 mg/ml. After another round of freezing/thawing and centrifugation, the final pellet was suspended in R buffer at 40 mg/ml. The purified lipid was frozen with liquid $N_2$ and stored at −80 °C until use.

The $K^+$ levels in the lipid suspensions in the purification above were monitored by an atomic absorption spectrophotometer (Z-2310, Hitachi). To an appropriately diluted lipid sample, we added KCl at 0, 0.01, 0.02, 0.03, and 0.04 mM. The absorbance increased linearly, giving the concentration of contaminant $K^+$ as the intercept. The contaminant $K^+$ was proportional to lipid (supplemental Fig. S2*B*), as expected. At 6 mg/ml of lipid during the acidification stage of the ATP synthesis assay, contaminant $K^+$ would be ~0.05 mM, which is negligible. The purification resulted in ~100-fold reduction of contaminant $K^+$ (supplemental Fig. S2*A*). The loss of lipid during the $K^+$ removal procedure was negligible, as checked by the EnzyChrom phospholipid assay kit (EPLP-100, BioAssay Systems).

*Reconstitution of $TF_oF_1$ into Liposomes and Acidification*—$TF_oF_1$ was reconstituted into liposomes as described (27) with the following modifications. To 250 μl of the purified lipid (40 mg/ml) in R buffer, we added 250 μl of a solution containing 0.8 M sucrose, 8% (w/v) *n*-octyl-β-D-glucoside (Dojindo), and 100 mM in total of KCl and NaCl at a desired ratio. We then mixed 75 μg of $TF_oF_1$. To the mixture, we added 200 μl of Biobeads SM-2 (Bio-Rad), which had been pre-equilibrated with 20 mM Tricine, 20 mM MES, 2.5 mM $MgCl_2$, and 50 mM of KCl+NaCl at the same ratio above, pH adjusted with NaOH to 8.0. The bead mixture was stirred gently for 30 min at 25 °C, and 300 μl of Biobeads were supplemented to the mixture. After another 2-h incubation, the suspension, now containing proteoliposomes, was transferred to a new tube, leaving the Biobeads behind.

For acid-base transition and formation of $K^+$-valinomycin diffusion potential, we first acidified the proteoliposomes at a desired pH in the presence of valinomycin and the desired concentration of $K^+$. 30 μl of the reconstituted proteoliposome suspension was mixed with 70 μl of acidic buffer (50 mM MES or HEPES or Tricine depending on pH, 14.7 mM $NaH_2PO_4$, 5 mM $MgCl_2$, 50 mM KCl+NaCl at the desired ratio, 0.6 M sucrose, pH adjusted with NaOH to 5.0–8.9) containing 0.7 mM ADP (A2754, Sigma) and 0.3 μM fresh valinomycin (V0627, Sigma). The suspension was incubated for 10–20 h at 23–27 °C. For incubation at pH > 8.4, $P_i$ in the acidic buffer was omitted to avoid sedimentation of MgPi. Increasing the valinomycin concentration 10- or 100-fold did not change the rate of synthesis. Mixture compositions are summarized in Table 1.

*ATP Synthesis Assay and Data Analysis*—ATP synthesis by $TF_oF_1$ was detected by luciferin-luciferase assay in a luminometer (Luminescencer AB2200, ATTO) equipped with a sample injection apparatus. We prepared a basic medium, to which the acidified proteoliposomes were to be injected, by mixing 21 μl of luciferin-luciferase medium (2× concentration, ATP bioluminescence assay kit CLSII, Roche Applied Science) supplemented with 3 mM luciferin (L9504, Sigma), 870 μl of basic buffer (350 mM HEPES or MOPS or Tricine depending on pH, 10 mM $NaH_2PO_4$, 5 mM $MgCl_2$, 50 mM KCl+NaCl, and 272 mM KOH+NaOH both at desired ratios), and 9 μl of 50 mM ADP (Table 1). At pH during the synthesis assay ($pH_{out}$) of 7.8, HEPES and MOPS gave the same rate of ATP synthesis, and HEPES and Tricine were indistinguishable at $pH_{out}$ of 8.0. The basic medium (900 μl) was incubated at 30 °C for 4 min in the luminometer, and then ATP synthesis reaction was initiated by

**TABLE 1**

**Summary of mixture compositions at three stages of incubation**

The compositions shown are those during incubation, after all components were mixed. The reconstitution column indicates the 2.5-h incubation with Biobeads in which proteoliposomes were formed; the acidification column indicates the 10–20-h incubation that was apparently sufficient for equilibration of pH and $[K^+]$ across the liposomal membranes; and the reaction column indicates the 60-s assay of ATP synthesis after the acidified proteoliposomes were mixed with the basic medium.

| | Reconstitution | Acidification | | | Reaction (outside liposomes) | | |
|---|---|---|---|---|---|---|---|
| | pH 8.0 | pH 5.6–6.8 | pH 7.0–8.0 | pH 8.2–8.8 | pH 7.2–7.8 | pH 8.0–8.2 | pH 8.4–8.8 |
| MES (mM) | 20 | 41 | 6 | 6 | 4.1 or 0.6 | 4.1 or 0.6 | 4.1 or 0.6 |
| Tricine (mM) | 20 | 6 | 6 | 41 | 0.6 | 0.6 | 305 or 309 |
| HEPES (mM) | 0 | 0 | 35 | 0 | 0 or 3.5 | 305 or 308 | 0 or 3.5 |
| MOPS (mM) | 0 | 0 | 0 | 0 | 305 | 0 | 0 |
| $MgCl_2$ (mM) | 2.5 | | 4.25 | | | 4.78 | |
| $NaH_2PO_4$ (mM) | 0 | | 10 | | | 9.73 | |
| KCl[a] (mM) | 0.1–50 | | 0.25–50 | | | 0.25–50 | |
| NaCl[a] (mM) | 50–0 | | 50–0 | | | 50–0 | |
| Sucrose[b] (mM) | 400 | | 540 | | | 54 | |
| KOH (mM) | 0 | | 0 | | | 0–231 | |
| NaOH (mM) | 30 | | 10–50 | | | 242–7 | |
| ADP[c] (mM) | 0 | | 0.5 | | | 0.5 | |
| Valinomycin (nM) | 0 | | 200 | | | 20 | |
| Osmolarity ($\times 10^{-3}$ osmol/liter) | 580 | | 730–770 | | | 750 | |

[a] [KCl] + [NaCl] = 50 mM, that is, $[Cl^-]$ = 50 mM in all stages (without counting $MgCl_2$).
[b] Osmolarity was balanced with sucrose.
[c] ADP contained 0.05 ± 0.01% of ATP as measured with the luciferin-luciferase assay.

the injection at time $t = 0$ of 100 μl of the acidified proteoliposome suspension. After 60 s, 10 μl of 10 μM ATP was added three times for calibration. The initial rate (at $t = 0$) of ATP synthesis was calculated from the exponential fit of the initial 0–6 s portion or 0–15 s when the rate of synthesis was low. All rate values reported in this work are the averages over three of more measurements on at least three independent reconstitutions, and the errors shown are the S.D. The pH of the acidified proteoliposome suspension and the pH of the reaction mixture were checked with a glass electrode for every condition and were reproducible. These values were taken as $pH_{in}$, the pH inside the liposomes, and $pH_{out}$, the pH outside liposomes. ΔpH is calculated as $pH_{out} - pH_{in}$. The transmembrane electrical potential Δψ is calculated from the Nernst equation, $\Delta\psi = (k_B T/e)\ln([K^+]_{out}/[K^+]_{in}) = 60.1 \cdot \log([K^+]_{out}/[K^+]_{in})$ in millivolts for our experiments at 30 °C, where $[K^+]_{in}$, the $K^+$ concentration inside the liposomes, is assumed to be that of the acidification mixture, in which lipid concentration was 6 mg/ml, and $[K^+]_{out}$ is taken as that of the reaction mixture. In the reaction mixture, $[TF_oF_1] = 8.5$ nM, [ADP] = 0.5 mM, $[P_i]$ = 10 mM, and [valinomycin] = 20 nM.

## RESULTS

*Measurement of ATP Synthesis Activity*—In this work, we used the $TF_oF_1$ lacking the inhibitory C-terminal domain of the ε subunit (28, 31). Hereafter, we refer to this mutant as $TF_oF_1$. $TF_oF_1$ was reconstituted into liposomes as before (27) with some modifications (see "Experimental Procedures"). The reconstitution and subsequent activity assay were highly reproducible; all of the experiments that we attempted contribute to the statistics below (every point in the graphs below shows the average over at least three assays on three or more independent reconstitutions, with the *error bar* showing the S.D.). In all reconstitutions, we used the same amounts of lipid (10 mg) and $TF_oF_1$ (75 μg); the weight ratio of 133:1 corresponds to two to three $TF_oF_1$ molecules per liposome for an assumed liposome diameter of 170 nm (27).

To drive ATP synthesis, we injected acidified proteoliposomes into a basic medium (acid base transition) to establish ΔpH, in the presence of valinomycin and $K^+$ that would generate a transmembrane voltage Δψ ($K^+$-valinomycin diffusion potential). Mixture compositions during reconstitution, acidification, and the final assay are summarized in Table 1. The concentrations of ADP and $P_i$, [ADP] and $[P_i]$, were 0.5 and 10 mM, respectively, which are saturating (27). The reaction temperature was 30 °C. The amount of ATP synthesized was monitored as the luminescence of the luciferin-luciferase system (Fig. 1). We allowed the synthesis reaction to proceed for 60 s and then added 0.1 nmol ATP three times to calibrate the luminescence signal. The luminescence was proportional to ATP up to 10 nmol (per 1 ml of reaction mixture). The synthesis reaction tended to level off as the imposed pmf decayed, so we fitted the initial portion with an exponential (*red lines* in Fig. 1) to estimate the initial rate that we report as the synthesis activity in this work. To express the activity as the turnover rate, we took all enzymes in the reaction mixture into account: no correction for the enzyme with the wrong orientation in the membrane, and thus, the rate values are underestimated.

The two sets of time courses in Fig. 1, one at varying ΔpH (Fig. 1*A*) and the other at varying Δψ (Fig. 1*B*), indicate that the (initial) rate of ATP synthesis is similar under the same pmf whether the pmf is dominated by ΔpH or Δψ. The overall time courses also appear similar in Fig. 1, but Δψ tends to decay faster than ΔpH as shown below. Nigericin, an $H^+$-$K^+$ antiporter, collapsed the pmf and prevented synthesis.

Before we proceed to detailed analyses, several remarks are in order. We calculate ΔpH as $pH_{out} - pH_{in}$ (see "Experimental Procedures"), where $pH_{in}$, the pH inside the proteoliposomes, is assumed to be the same as the pH of the proteoliposome suspension after incubation for acidification. To see whether equilibration across the liposomal membranes was reached during acidification, we changed the incubation time and tested the rate of synthesis (supplemental Fig. S1). The rate rose with incubation time and leveled off at ~6 h, so we chose the incubation time of 10–20 h in subsequent experiments.

The transmembrane electrical potential is calculated from the Nernst equation as $\Delta\psi = 60.1 \cdot \log([K^+]_{out}/[K^+]_{in})$ in millivolts (see "Experimental Procedures"). To avoid an osmotic imbalance, which would change $[K^+]_{in}$, we minimized the difference in the osmolarities of the acidification and reaction mixture with sucrose (Table 1). The Nernst equation above is valid when the transmembrane flux of $K^+$ far exceeds fluxes of other ions (hence we added valinomycin, a $K^+$ carrier). We checked this by changing $[K^+]$ as described below.

Another problem with regard to calculating $\Delta\psi$ was the $K^+$ contamination in the lipid, which amounted to ~5 mM at 6 mg lipid/ml (supplemental Fig. S2), the lipid concentration during acidification where we set $[K^+]_{in}$. Lipids of higher purity from Avanti or Lipoid company contained much less (but non-negligible) $K^+$, but the rate of ATP synthesis was several times lower than with the crude lipid we used. We therefore washed the crude lipid in five cycles of centrifugation and freezing/thawing, reaching the contaminant $K^+$ level of ~0.05 mM in 6 mg/ml lipid suspension as measured by atomic absorption (supplemental Fig. S2). $[K^+]$ in other reagents was <30 μM in total.

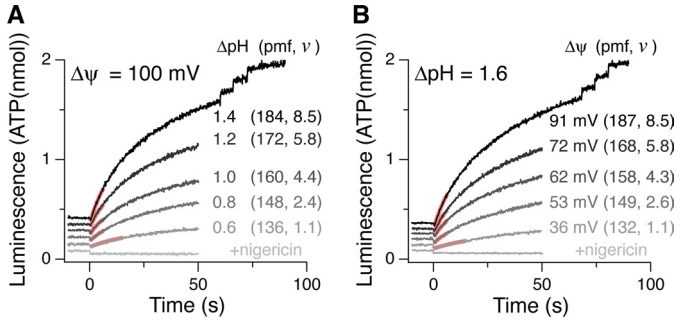


FIGURE 1. **Time courses of ATP synthesis at different pmf (in mV).** Synthesis reaction was initiated by the injection of acidified proteoliposomes at $t = 0$. Vertical axes show the intensity of luciferin luminescence, which was converted to the amount of ATP in the reaction mixture by three additions of 0.1 nmol of ATP after $t = 60$ s. The initial rate of synthesis, $v$ (in $s^{-1}$), was calculated from the exponential fit over 0–6-s or 0–15-s portions (*red curves*). $[K^+]_{in} = 5$ mM; $pH_{out} = 8.0$. *A*, ΔpH dependence at Δψ of 100 mV ($[K^+]_{out} = 237$ mM; $pH_{in} = 7.4$ to 6.6). Nigericin was added at ΔpH of 2.0. *B*, Δψ dependence at ΔpH of 1.6 ($pH_{in} = 6.4$; $[K^+]_{out} = 21$ to 162 mM). Nigericin at $\Delta\psi = 100$ mV.

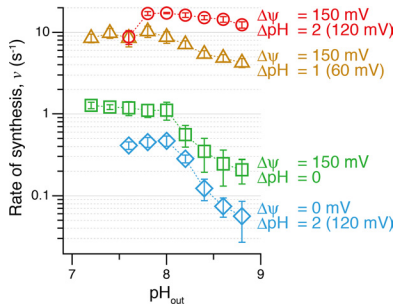


FIGURE 2. **pH dependence of the initial rate of ATP synthesis, *v*, under constant ΔpH and Δψ as indicated.** $[K^+]_{out} = 180$ mM and $[K^+]_{in} = 0.5$ mM except for *diamonds* where $[K^+]_{out} = [K^+]_{in} = 50$ mM. Δψ values shown are nominal values based on the Nernst equation.

*pH Dependence of ATP Synthesis*—To change ΔpH in appropriate fashions, we first inquired how the rate of ATP synthesis depends on $pH_{out}$ and $pH_{in}$ themselves. The pmf we imposed was always inside positive, and thus, those synthase molecules with the $F_1$ portion outside the liposome were engaged in synthesis. That is, the synthesis reaction proceeded at $pH_{out}$.

We applied constant ΔpH and Δψ while changing $pH_{out}$ and $pH_{in}$ simultaneously (Fig. 2). At $pH_{out}$ between 7.2 and 8.0, the synthesis rate was independent of $pH_{out}$ (and $pH_{in}$). Exceptions were the leftmost points of the top and bottom curves at $pH_{out} = 7.6$, where $pH_{in}$ was 5.6. We consistently observed a drop in the synthesis activity when $pH_{in}$ was decreased from 5.8 to 5.6 for an unknown reason. We did not explore the cause (possibly acid denaturation) because with MES used for buffering, we could not decrease $pH_{in}$ below 5.5. At $pH_{out}$ above 8.0, on the other hand, the activity decreased with $pH_{out}$ particularly at low pmf (lower curves), a possible reason being the increase of the free energy for ATP synthesis at higher pH (32). To study pmf dependence while minimizing the effect of pH itself, experiments below were carried out at $pH_{out}$ of 8.0, unless stated otherwise, and $pH_{in}$ above 5.6 (data at $pH_{in} = 5.6$ are included as a reference).

*Kinetic Equivalence of ΔpH and Δψ*—The ΔpH dependence of the rate of ATP synthesis at various Δψ and at the constant $pH_{out}$ of 8.0 is summarized in Fig. 3*A* (*closed circles*). The drop

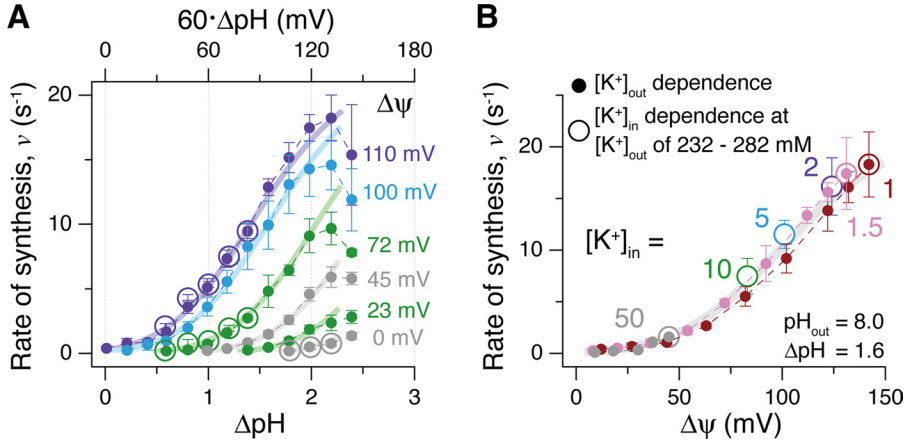


FIGURE 3. **Dependence of the initial rate of ATP synthesis, *v*, on ΔpH, Δψ, and $[K^+]$.** *A*, ΔpH dependence at different Δψ. *Closed circles*, $pH_{in}$ varied from 8.0 to 5.6 at $pH_{out} = 8.0$; *open circles*, $pH_{out}$ varied from 8.0 to 7.2 at $pH_{in} = 6.6$. *Colors* indicate $[K^+]_{in}$ as defined in *B*. *B*, $[K^+]$ dependence at ΔpH of 1.6. *Closed circles*, $[K^+]_{out}$ varied from 1 to 232–282 mM at constant $[K^+]_{in}$ of 1, 1.5, and 50 mM (shown in different colors); *open circles*, $[K^+]_{in}$ varied from 1 to 50 mM (color-coded) at $[K^+]_{out}$ of 232–282 mM.

in rate at the rightmost points (ΔpH = 2.4) is due to the low $pH_{in}$ of 5.6 as stated above. All points except for the rightmost ones fall on thick smooth lines that represent the consensus pmf dependence (*gray line* in Fig. 4*A*), indicating that the synthesis activity is determined by pmf, irrespective of the relative contributions of ΔpH and Δψ. *Open circles* in Fig. 3*A* show the activities at different $pH_{out}$ between 7.2–8.0, confirming that $pH_{out}$ does not affect the activity in this range (Fig. 2).

To vary Δψ in experiments in Fig. 3*A*, we changed $[K^+]_{in}$ (and $[K^+]_{out}$) as indicated by color. If the Nernst equation holds, Δψ should depend only on the ratio, $[K^+]_{out}/[K^+]_{in}$. To confirm this, we measured the rate of synthesis at constant $[K^+]_{in}$ of 1 mM, 1.5 mM or 50 mM while changing $[K^+]_{out}$ to vary Δψ (*closed circles* in Fig. 3*B*) or kept $[K^+]_{out}$ within 232–282 mM while varying $[K^+]_{in}$ (*open circles*). The results again fall on the consensus line (*thick gray curve*), indicating that Δψ is determined by the ratio $[K^+]_{out}/[K^+]_{in}$. Below $[K^+]_{in}$ of 1 mM, we observed apparent deviations from the consensus curve, which we ascribe to contribution of ion fluxes other than $K^+$ (supplemental Figs. S3 and S4).

In Fig. 4, we plot all activity data, including those not shown in Fig. 3 and excluding those at $[K^+]_{in} < 1$ mM or at $pH_{in} = 5.6$. As seen in Fig. 4*A*, all activity values are the function of pmf alone, irrespective of whether ΔpH or Δψ was varied or of $[K^+]_{in}$ (1–50 mM, indicated by different colors). The combinations of ΔpH and Δψ tested are shown in Fig. 4*B*, ΔpH ranging between −0.3 and 2.2 and Δψ ranging between −30 and 140 mV. In Fig. 4*B*, the activity values are represented by colors, and the diagonal distribution attests to the kinetic equivalence of ΔpH and Δψ in ATP synthesis in the ranges shown.

*ATP Synthesis by ΔpH or Δψ Alone*—Of particular concern to the equivalence of ΔpH and Δψ is whether ΔpH or Δψ alone suffices for ATP synthesis and, if so, whether the two show similar rates of synthesis. The time courses in Fig. 5*A* show that, indeed, either alone can drive ATP synthesis. The synthesis rates were not high, but this was because we could not apply a high enough pmf: ΔpH was limited to 2.2 and the condition $[K^+]_{in} \geq 1$ mM limited Δψ to below ~140 mV. The most important observation is that either ΔpH or Δψ drove synthesis even when the other opposed (*traces iii* and *vii* in Fig. 5*A*).

The rates of synthesis are compared in Fig. 5*B* as functions of pmf, indicating kinetic equivalence of ΔpH alone and Δψ alone. Superposition of negative Δψ on ΔpH of 2.2 (*gray open circles*) or negative ΔpH on Δψ of 131 mV (*magenta open squares*) gave expected rates. That is, equivalence of ΔpH and Δψ holds irrespective of their signs, or the contributions of ΔpH and Δψ to pmf are additive as an algebraic sum. The data in Fig. 5 are included in Fig. 4.

In Fig. 5*A*, we note that the rate of synthesis slowed down faster with Δψ than with ΔpH. Whereas pH was buffered both inside and outside the liposomes, we could not buffer $[K^+]$. Leakage of ions other than $K^+$ breaks the $K^+$ equilibrium across the membrane and an influx of $K^+$ would ensue. As expected,

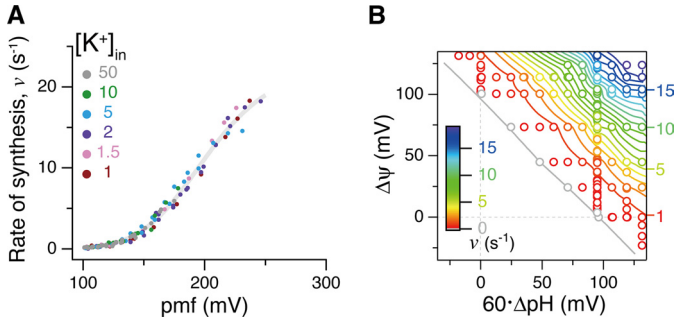


FIGURE 4. **Kinetic equivalence of ΔpH and Δψ for ATP synthesis.** *A*, all rate data obtained at $pH_{in}$ of 5.8 to 8.0, $pH_{out}$ of 7.2 to 8.0, and $[K^+]_{in} \geq 1$ mM. *Error bars* are omitted for clarity. The *gray curve* is an arbitrary fit with $v = v_0/[1 + (p_0/p)^q]$, where $p$ = pmf, $p_0$ = 202 mV, $q$ = 7.18, and $v_0$ = 23.1 $s^{-1}$. *B*, contour representation of ΔpH and Δψ dependence. *Small circles* show data points and synthesis rates are color-coded.

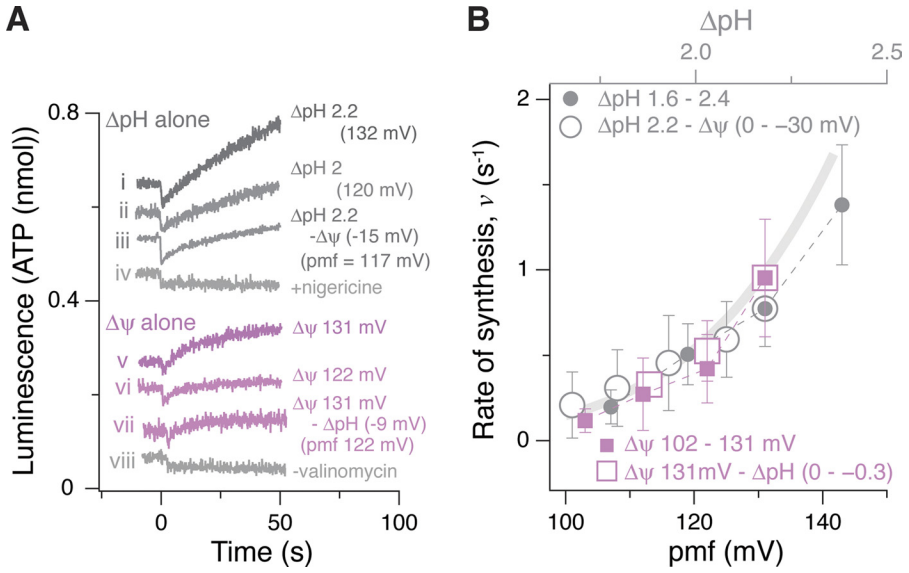


FIGURE 5. **ATP synthesis driven by either ΔpH or Δψ alone.** *A*, time courses of synthesis. *Traces i–iv*, ΔpH alone (Δψ = 0) except for *trace iii*; *traces v–viii*, Δψ alone (ΔpH = 0) except for *trace vii*. 500 nM nigericin was added (*trace iv*) to *trace i*, and valinomycin was eliminated (*trace viii*) from *trace v*. *B*, summary of the synthesis activity against pmf. *Closed gray circles*, ΔpH alone at $[K^+]_{out} = [K^+]_{in} = 50$ mM; *open gray circles*, negative Δψ added to ΔpH of 2.2 by decreasing $[K^+]_{out}$ from 50 down to 12 mM; *Closed magenta squares*, Δψ alone at $[K^+]_{in} = 1.5$ mM and $[K^+]_{out}$ from 76 to 233 mM; *open magenta squares*, negative ΔpH was added to Δψ of 131 mV by decreasing $pH_{out}$ from 8.0 down to 7.7 at fixed $pH_{in}$ of 8.0. $pH_{out} = 8.0$ except for the *open magenta squares*.

the deceleration of synthesis (decay of $\Delta\psi$) was faster for lower $[K^+]_{in}$ (supplemental Fig. S3). Faster decay of $\Delta\psi$ has been documented (33, 34).

## DISCUSSION

We have tested many combinations of ΔpH and $\Delta\psi$, including negative values, and have observed kinetic equivalence for the ranges we were able to explore. Synthesis appeared to begin at pmf of ~100 mV (Fig. 4). In our experiments, [ADP] and $[P_i]$ were controlled to 0.5 mM and 10 mM, respectively, and ADP contained 0.25±0.05 μM of contaminant ATP as assessed by the luciferase assay. The Gibbs free energy of the phosphorylation of ADP at $pH_{out}$ of 8.0 has been measured with chloroplast $F_oF_1$ to be 37 kJ/mol (35), and the number of *c* subunits in our *Bacillus* PS3 $F_oF_1$ is 10 (36), implying an $H^+$/ATP ratio of 3.3. These values imply that the synthesis and hydrolysis would be balanced at pmf of ~95 mV. The starting value of ~100 mV is consistent with this calculation. The equivalence of ΔpH and $\Delta\psi$ has been shown mostly at $pH_{out}$ of 8.0, but limited data including those in Fig. 2 and 3A suggest that the equivalence holds at least down to $pH_{out}$ of 7.2. In bacteria, the $F_1$ portion is on the intracellular side and thus, contrary to our proteoliposome system, ATP synthesis occurs inside the bacterium, where the pH is ~7.5 (37). The implication is that the kinetic equivalence may well be physiological, although the optimal temperature of our thermophilic enzyme is ~60 °C or above, whereas the experiments described here were made at 30 °C.

The demonstration of kinetic equivalence over the wide ranges of ΔpH and $\Delta\psi$ depended on several key factors. First, presumably due to the removal of the inhibitory domain of the ε subunit, we did not encounter a serious activation problem. As noted under the Introduction, $F_oF_1$ from other sources is often partially dormant and its activation may be promoted by ΔpH and/or $\Delta\psi$. Second, careful removal of contaminant $K^+$ from the lipid allowed control of $[K^+]_{in}$ to the precision of 0.1 mM or below. We also avoided an osmotic imbalance, which would affect $[K^+]_{in}$. Because $[K^+]_{out}$ cannot be arbitrarily high, we had to work at a low $[K^+]_{in}$ to obtain high $\Delta\psi$. Our data indicate that the straightforward use of the Nernst equation is valid down to $[K^+]_{in}$ as low as ~1 mM (Fig. 4; also see supplemental Figs. S3 and S4). This would not be the case without the precise control of $K^+$ concentrations. Third, we incubated the acidified proteoliposomes for >10 h to ensure equilibration of $H^+$ (and buffer) and $K^+$ across the membrane (supplemental Fig. S1). With a buffer such as succinate, the apparent equilibration was much faster (minutes), but a highly permeable buffer may pose a problem (38), and thus, we chose to use Good's buffers. Except for the saturation of the rate of synthesis with the incubation time (supplemental Fig. S1), we did not confirm the equilibration during acidification directly. An indirect but strong support is the overlap of all data points on the single consensus curve (Fig. 4*A*). Fourth, we fixed $pH_{out}$, the pH at which the phosphorylation of ADP takes place, to 8.0 (down to 7.2 in some experiments), after confirming that the rate of synthesis is constant between 7.2–8.0 (Fig. 2). The phosphorylation reaction *per se* is pH-dependent (32, 39), which must be distinguished from the effect of ΔpH. We also removed the data at $pH_{in}$ of 5.6 in Fig. 4 because, at this $pH_{in}$, the rate was lower irrespective of $pH_{out}$.

ATP synthesis has been demonstrated at the single-molecule level (11, 12), but without the $F_o$ portion (without the proton motive force). Proton-driven rotation of $F_oF_1$ has been demonstrated experimentally (13), but so far up to at most a few turns. Development of a better *in vitro* system for single-molecule observation is desired for the elucidation of the mechanisms of proton-driven rotation and the coupling between rotation and ATP synthesis. We have been trying to develop a liposome-based system, so far without success (40). The kinetic equivalence we have shown here implies that, in a single-molecule observation system, one can use voltage, pH gradient, or any combination of the two to drive rotation at an equal efficiency. The freedom will certainly help design decisive experiments.

*Acknowledgments—We thank C. Wakabayashi for continuous support in $TF_oF_1$ purification, M. Bertz for an analysis program, members of the Kinosita and Yoshida Laboratories for help and advice, and S. Takahashi for encouragement and laboratory management.*

## REFERENCES

1. Deckers-Hebestreit, G., and Altendorf, K. (1996) The $F_0F_1$-type ATP synthases of bacteria: Structure and function of the $F_0$ complex. *Annu. Rev. Microbiol.* **50,** 791–824
2. Boyer, P. D. (1997) The ATP synthase–A splendid molecular machine. *Annu. Rev. Biochem.* **66,** 717–749
3. Weber, J., and Senior, A. E. (2003) ATP synthesis driven by proton transport in $F_1F_0$-ATP synthase. *FEBS Lett.* **545,** 61–70
4. Yoshida, M., Muneyuki, E., and Hisabori, T. (2001) ATP synthase–A marvelous rotary engine of the cell. *Nat. Rev. Mol. Cell Biol.* **2,** 669–677
5. Junge, W., Sielaff, H., and Engelbrecht, S. (2009) Torque generation and elastic power transmission in the rotary $F_0F_1$-ATPase. *Nature* **459,** 364–370
6. Dimroth, P., von Ballmoos, C., and Meier, T. (2006) Catalytic and mechanical cycles in F-ATP synthases. Fourth in the Cycles Review Series. *EMBO Rep.* **7,** 276–282
7. Abrahams, J. P., Leslie, A. G., Lutter, R., and Walker, J. E. (1994) Structure at 2.8 A resolution of $F_1$-ATPase from bovine heart mitochondria. *Nature* **370,** 621–628
8. Boyer, P. D., and Kohlbrenner, W. E. (1981) in *Energy Coupling in Photosynthesis*, pp. 231–240, Elsevier B.V., Amsterdam
9. Oosawa, F., and Hayashi, S. (1986) The loose coupling mechanism in molecular machines of living cells. *Adv. Biophys.* **22,** 151–183
10. Noji, H., Yasuda, R., Yoshida, M., and Kinosita, K., Jr. (1997) Direct observation of the rotation of $F_1$-ATPase. *Nature* **386,** 299–302
11. Itoh, H., Takahashi, A., Adachi, K., Noji, H., Yasuda, R., Yoshida, M., and Kinosita, K., Jr. (2004) Mechanically driven ATP synthesis by $F_1$-ATPase. *Nature* **427,** 465–468
12. Rondelez, Y., Tresset, G., Nakashima, T., Kato-Yamada, Y., Fujita, H., Takeuchi, S., and Noji, H. (2005) Highly coupled ATP synthesis by $F_1$-ATPase single molecules. *Nature* **433,** 773–777
13. Düser, M. G., Zarrabi, N., Cipriano, D. J., Ernst, S., Glick, G. D., Dunn, S. D., and Börsch, M. (2009) 36° step size of proton-driven *c*-ring rotation in $F_oF_1$-ATP synthase. *EMBO J.* **28,** 2689–2696
14. Diez, M., Zimmermann, B., Börsch, M., König, M., Schweinberger, E., Steigmiller, S., Reuter, R., Felekyan, S., Kudryavtsev, V., Seidel, C. A., and Gräber, P. (2004) Proton-powered subunit rotation in single membrane-bound $F_0F_1$-ATP synthase. *Nat. Struct. Mol. Biol.* **11,** 135–141
15. Börsch, M., and Gräber, P. (2005) Subunit movement in individual $H^+$-ATP synthases during ATP synthesis and hydrolysis revealed by fluorescence resonance energy transfer. *Biochem. Soc. Trans.* **33,** 878–882
16. Steigmiller, S., Turina, P., and Gräber, P. (2008) The thermodynamic $H^+$/

ATP ratios of the $H^+$-ATP synthases from chloroplasts and *Escherichia coli*. *Proc. Natl. Acad. Sci. U.S.A.* **105,** 3745–3750
17. Mitchell, P. (1961) Coupling of phosphorylation to electron and hydrogen transfer by a chemi-osmotic type of mechanism. *Nature* **191,** 144–148
18. Bokranz, M., Mörschel, E., and Kröger, A. (1985) Phosphorylation and phosphate-ATP exchange catalyzed by the ATP synthase isolated from *Wolinella succinogenes*. *Biochim. Biophys. Acta* **810,** 332–339
19. Slooten, L., and Vandenbranden, S. (1989) ATP-synthesis by proteoliposomes incorporating *Rhodospirillum rubrum* $F_0F_1$ as measured with firefly luciferase: Dependence on Δψ and ΔpH. *Biochim. Biophys. Acta* **976,** 150–160
20. Hangarter R. P., and Good N. E. (1982) Energy thresholds for ATP synthesis in chloroplasts. *Biochim. Biophys. Acta* **681,** 397–404
21. Junesch, U., and Gräber, P. (1991) The rate of ATP-synthesis as a function of ΔpH and Δψ catalyzed by the active, reduced $H^+$-ATPase from chloroplasts. *FEBS Lett.* **294,** 275–278
22. Wiedenmann, A., Dimroth, P., and von Ballmoos, C. (2009) Functional asymmetry of the $F_0$ motor in bacterial ATP synthases. *Mol. Microbiol.* **72,** 479–490
23. Turina, P. (1994) Influence of transmembrane electrochemical proton gradient on catalysis and regulation of the $H^+$-ATP synthase from *Rhodobacter capsulatus*. *Bioelectrochem. Bioenerg.* **33,** 31–43
24. Fischer, S., and Gräber, P. (1999) Comparison of ΔpH- and Δψ-driven ATP synthesis catalyzed by the $H^+$-ATPases from *Escherichia coli* or chloroplasts reconstituted into liposomes. *FEBS Lett.* **457,** 327–332
25. Iino, R., Hasegawa, R., Tabata, K. V., and Noji, H. (2009) Mechanism of inhibition by C-terminal α-helices of the ε subunit of *Escherichia coli* $F_oF_1$-ATP synthase. *J. Biol. Chem.* **284,** 17457–17464
26. Adachi, K., Furuike, S., Hossain, M. D., Itoh, H., Kinosita, K., Jr., Onoue, Y., and Shimo-Kon, R. (2010) in *Single Molecule Spectroscopy in Chemistry, Physics and Biology*, pp. 271–285, Springer-Verlag, Berlin
27. Soga, N., Kinosita, K., Jr., Yoshida, M., and Suzuki, T. (2011) Efficient ATP synthesis by thermophilic *Bacillus* $F_oF_1$-ATP synthase. *FEBS J.* **278,** 2647–2654
28. Masaike, T., Suzuki, T., Tsunoda, S. P., Konno, H., and Yoshida, M. (2006) Probing conformations of the β subunit of $F_0F_1$-ATP synthase in catalysis. *Biochem. Biophys. Res. Commun.* **342,** 800–807
29. Suzuki, T., Murakami, T., Iino, R., Suzuki, J., Ono, S., Shirakihara, Y., and Yoshida, M. (2003) $F_0F_1$-ATPase/synthase is geared to the synthesis mode by conformational rearrangement of ε subunit in response to proton motive force and ADP/ATP balance. *J. Biol. Chem.* **278,** 46840–46846
30. Kagawa, Y., and Racker, E. (1971) Partial resolution of the enzymes catalyzing oxidative phosphorylation. *J. Biol. Chem.* **246,** 5477–5487
31. Suzuki, T., Wakabayashi, C., Tanaka, K., Feniouk, B. A., and Yoshida, M. (2011) Modulation of nucleotide specificity of thermophilic $F_oF_1$-ATP synthase by ε subunit. *J. Biol. Chem.* **286,** 16807–16813
32. Rosing, J., and Slater, E. C. (1972) The value of ΔG° for the hydrolysis of ATP. *Biochim. Biophys. Acta* **267,** 275–290
33. Blok, M. C., De Gier, J., and Van Deenen, L. L. (1974) Kinetics of the valinomycin-induced potassium ion leak from liposomes with potassium thiocyanate enclosed. *Biochim. Biophys. Acta* **367,** 210–224
34. Wiedenmann, A., Dimroth, P., and von Ballmoos, C. (2008) Δψ and ΔpH are equivalent driving forces for proton transport through isolated $F_0$ complexes of ATP synthases. *Biochim. Biophys. Acta* **1777,** 1301–1310
35. Turina, P., Samoray, D., and Gräber, P. (2003) $H^+$/ATP ratio of proton transport-coupled ATP synthesis and hydrolysis catalyzed by $CF_0F_1$-liposomes. *EMBO J.* **22,** 418–426
36. Mitome, N., Suzuki, T., Hayashi, S., and Yoshida, M. (2004) Thermophilic ATP synthase has a decamer *c*-ring: Indication of noninteger 10:3 $H^+$/ATP ratio and permissive elastic coupling. *Proc. Natl. Acad. Sci. U.S.A.* **101,** 12159–12164
37. Cook, G. M. (2000) The intracellular pH of the thermophilic bacterium *Thermoanaerobacter wiegelii* during growth and production of fermentation acids. *Extremophiles* **4,** 279–284
38. Kaim, G., and Dimroth, P. (1999) ATP synthesis by F-type ATP synthase is obligatorily dependent on the transmembrane voltage. *EMBO J.* **18,** 4118–4127
39. Förster, K., Turina, P., Drepper, F., Haehnel, W., Fischer, S., Gräber, P., and Petersen, J. (2010) Proton transport coupled ATP synthesis by the purified yeast $H^+$-ATP synthase in proteoliposomes. *Biochim. Biophys. Acta* **1797,** 1828–1837
40. Onoue, Y., Suzuki, T., Davidson, M., Karlsson, M., Orwar, O., Yoshida, M., and Kinosita, K., Jr. (2009) A giant liposome for single-molecule observation of conformational changes in membrane proteins. *Biochim. Biophys. Acta* **1788,** 1332–1340